Aerosol mediated localized dissolution to enhance the electrical behavior and sensitivity of piezoresistive nanofiber-based flexible sensors

Applied Materials Today 33 (2023) 101863

Contents lists available at ScienceDirect

Applied Materials Today

journal homepage: www.elsevier.com/locate/apmt

Aerosol mediated localized dissolution to enhance the electrical behavior and sensitivity of piezoresistive nanofiber-based flexible sensors

Marzia Quaglio [a,b,*], Candido F. Pirri [a,b], Giulia Massaglia [a,b,*]

[a] Department of Applied Science and Technology, Politecnico di Torino, Corso Duca degli Abruzzi 24, 10129 Torino, Italy
[b] Centre for Sustainable Future and Technologies @ Polito, Istituto Italiano di Tecnologia, Via Livorno 60, Torino, 10100, Italy

ARTICLE INFO

Keywords:
Electrospinning
Nanofibers
Wearable sensors
Inter-fibers melting
Piezoresistive nanocomposites

ABSTRACT

This work proposes the use of solvents in the form of small size droplets to improve the connections among nanofibers (NFs) in electrospun composite nanofibers with carbon nanotube multiwalled (MWCNT) by improving the electrical and piezoresistive behavior of such electrically conductive polymer composites. The here proposed Aerosol Mediated Localized Dissolution (AMLD) process has been shown to be effective in improving the 3D microporous NF mat by inducing local dissolution that is effective in improving the connections among fibers within the mat. The AMLD process is demonstrated here for polyethylene oxide (PEO) / MWCNTs composite nanofibers, showing that the electrical conductivity is particularly improved in those samples with low content of MWCNTs, even below the original percolation threshold. The improved electrical conductivity is coupled with exceptional sensitivity of the flex sensor for low MWCNTs contents, this is particularly due to the ability of the AMLD process to preserve the high surface area of the 3D mat by inducing better fiber-to-fiber contacts in few regions only. In addition, this work demonstrates the effectiveness of applying an electrical potential difference during the AMLD process to improve the alignment of MWCNTs within the 3D microporous NF mat. The combination of voltage and AMLD allow to obtain a gauge factor as high as 571.9 with a MWCNTs loading of 1 wt%.

1. Introduction

In recent decades, electrically conductive polymer composites (ECPCs) have received much attention from the scientific and engineering communities for their ability to fuse mechanical and electrical properties into unique piezoresistive behaviors [1]. In ECPCs, electrically conductive fillers are added to a nonconductive polymer matrix: if the filler content exceeds a threshold value, a conductive network is formed throughout the insulating polymer matrix. The level of electrical conductivity of ECPCs is strictly related not only to the concentration of the filler, but also to its shape and size, with a significant improvement of the final behavior when nanostructured fillers are used [2]. Nanostructured materials, as carbon nanotubes, carbon and metallic nanoparticles, and 2D materials have been successfully introduced minimizing the required filler concentration and improving the final behavior of the materials [3–6], thus achieving ECPCs with higher sensitivity with respect to piezoresistive materials with traditional fillers.

Improvements on ECPCs have contributed significantly to the development of new classes of flexible and stretchable strain and pressure sensors useful for exciting applications in health monitoring, human motion detection, augmented reality, electronic skins [7,8].

Further improvements of piezoresistive sensors have been possible by transforming flexible continuous sensing films into 3D microporous structures that can improve the pressure sensing performance of the device. The design and fabrication of flexible 3D microporous materials offers a unique opportunity to increase the surface area of the material, increasing the likelihood of changing electrical pathways when pressure is applied to the sensing material [9–19]. Among the possible approaches to produce 3D microporous structure, electrospinning is one of the most attractive methods to couple effective polymer matrix nanostructuring with traditional strategies to design exceptional ECPCs. In fact, with respect to traditional ECPSs nanocomposites characterized by a continuous matrix, electrospinning enables to design lightweight and flexible nanofiber mats from polymer solutions with dispersed inorganic nanofillers such as carbon nanotubes [20–24].

Electrospinning is an electrohydrodynamic process whose working principle is based on the ability of strong repulsive electrical forces to

* Corresponding authors.
E-mail addresses: marzia.quaglio@polito.it (M. Quaglio), giulia.massaglia@polito.it (G. Massaglia).

https://doi.org/10.1016/j.apmt.2023.101863
Received 18 January 2023; Received in revised form 12 May 2023; Accepted 5 June 2023
Available online 17 June 2023

overcome the surface tension in a charged polymeric jet [25]. The resulting polymeric nanofibers are collected into porous mats characterized by high surface area to volume ratio [26–29]. This technology is extremely versatile as it allows polymeric solutions of natural and synthetic polymers to be processed and polymer mats to be converted into metal oxides, ceramics, metals, and composite nanomaterials [30–34].

The porosity characterizing the nanofiber mats is critical for the most part of applications [35,36]. Unfortunately, porosity is usually associated to an open structure with a low degree of connection among nanofibers, and this can significantly limit the properties of the resulting mats, particularly by reducing both in-plane and out-of-plane transport and conduction phenomena [37,38]. In electrochemistry and water filtration, electrospun nanofiber mats are usually treated by thermal and/or solvent-assisted processes, usually combined with mechanical compression, to increase the degree of connection among nanofibers [37–39]. With these approaches, the improvement in transport properties is unfortunately combined with a decrease of the overall internal porosity of the nanofiber mats. The reduction of porosity is inherently associated with compression-based processes for forming inter-fiber junctions and may limit the applicability of the obtained materials in other fields, as it may worsen the mechanical behavior of the mats. In cell culture technology, the problem can be overcome by post-compression treatments to create new pores in the proper size range [40,41]. More recently, a thermal bonding procedure that does not require the application of pressure has been shown to be effective in enhancing inter-fibers bonds [42]. However, even without the application of pressure, heat treatments at temperatures in the range between the glass transition and the melting temperature significantly compromise the porosity of the starting mats.

A proper balance between large surface area and large number of fiber-to-fiber connections plays a key role in determining the final properties of nanofiber mats, in terms of large surface area and electrical conductivity, necessary to design exceptional piezoresistive properties for wearable sensors [7]. Indeed, considering composite nanofibers made of skin-compatible polymers and multiwall carbon nanotubes as the electrically conducting nanofiller [3], the fabrication of a three-dimensional mat with excellent behavior requires large surface area associated with open pores to improve mechanical properties in terms of compressibility, elasticity, and flexibility, and large number of fiber-to-fiber connections to ensure rapid electrical transduction [43].

This work proposes the use of solvents in the form of small size droplets to induce local enhancement of fiber-to-fiber connections while preserving the original porosity of the electrospun material in the regions not reached by the droplets. Among the various approaches available to atomize solvents, we chose ultrasonic aerosol in this work. The resulting process, called Aerosol Mediated Localized Dissolution (AMLD), aims to achieve control over the morphology of the 3D nanofibrous materials by inducing a hybrid structure in the treated mat, in which a small number of modified regions form in a predominantly unmodified 3D microporous mat. In this work, composite nanofibers of polyethylene oxide (PEO) and multi-walled carbon nanotubes (MWCNTs) were chosen as a model material for two main reasons: i) their electrical behavior is based on a percolation process [44] and is therefore particularly sensitive to the arrangement of the nanofibers in the mat; ii) the high skin compatibility of PEO, which makes this polymer an ideal choice for wearable applications [45,46]. In this scenario, composite nanofibers based on PEO and MWCNTs can be very representative to demonstrate the potential of the AMLD process for highly sensitive flexible sensors.

In the present work, the central role of AMLD in improving the electrical and piezoresistive behavior of the 3D microporous NF hybrid mat is first demonstrated in terms of the enhanced electrical conductivity of the PEO/MWCNTs composite nanofibers. The electrical conductivity is particularly improved in samples with low MWCNT content, even below the original percolation threshold, and this is particularly related to the improved percolation pathway achieved by increasing the number of fiber-to-fiber connections. The improvement in electrical conductivity is accompanied by an extraordinary sensitivity of the flex sensor for low MWCNTs contents, mainly due to the ability of the AMLD process to preserve the high surface area of the 3D mat, inducing an improvement of the fiber-to-fiber contacts only in certain regions. Moreover, this work demonstrates the effectiveness of applying an electrical potential difference during the AMLD process. The combination of voltage and local dissolution allows exploiting the mobility of MWCNTs into the dissolving regions [47,48], achieving further improvement of the electrical conductivity by rearranging MWCNTs.

2. Materials and methods

2.1. Synthesis of polymeric composite nanofibers

Water-based solutions were prepared by adding 5 wt% PEO with an average molecular weight of 1000 kDa (purchased from Sigma Aldrich). The solutions were then aged overnight under continuous stirring at room temperature. Composite conductive nanofibers were obtained by adding MWCNTs to the PEO solutions. The complete process flow is the same as that reported by Massaglia et al. [44].

MWCNTs (NC3100 by Nanocyl) with purity ~95% and 1.5 μm long, were dispersed by ultrasonic bath (2000U Digital Sonifier by Branson) in solutions of DI water and sodium polystyrene sulfonate (Na-PSS, Sigma Aldrich), with a Na-PSS to MWCNTs molar ratio equal to 1. Weight percentages of functionalized MWCNTs were used, ranging from 1 to 7 wt%. The final electrospinning solutions were obtained by mixing the two water-based solutions, the one containing PEO and the one with MWCNTs, and aged un-der continuous stirring overnight at room temperature.

The polymeric solution was appropriately loaded into a syringe for the electrospinning process. A NANON 01A equipment by MECC was used, allowing the selection of flow rates in the range (0.1 - 99.9) ml/hr and fixing the operating voltage in the range from 0.5 kV to 30 kV. Disposable plastic syringes with a volume of 6 ml, connected to a 27 Gauge x 15 mm needle, were used. Aluminum foils were used as reference substrates during process optimization, and glass slides were used for electrical characterizations to collect the nanofibers. In agreement with the results obtained from our previous work, [44] we selected PEO with a higher molecular weight with the main objective to obtain a denser nanofiber netting, which played a pivotal role to enhance the electrical conductivity of the final composite nanofibers.

Aerosol treatment was carried out with a Clenny A Family system, by Chiesi. Also, in the present work, given the high solubility of PEO in water, the solvent atomized by AMLD process is deionized water.

2.2. Nanofibers characterizations

Field Effect Scanning Electron Microscopy (FESEM) by Zeiss Merlin was used to deeply analyse the morphology of the nonwoven mats.

Glass slides were used as substrates to fabricate the samples for electrical characterizations. Hard-masks, made of poly(methyl)methacrylate PMMA were fabricated by column CNC milling machine and, by placing them on the glass slides, were used both to prepare the electrodes and to pattern the nanofibers mats for the electrical characterizations. Nanofiber strips, having a length of 2 cm and a width of 2 mm, were prepared with hard-mask.

A Tencor P-10 Surface Profiler was used to evaluate the thickness of the nanofiber strips, and FESEM analysis on the samples analysed in cross section helped confirm the values. Four Au electrodes were obtained on each nanofiber strip by sputtering with a current of 50 mA for 120 s (Q150T ES by Quorum Technologies) in presence of a hard-mask. Platinum films 100 nm thick, 1 mm wide and 5 mm long were fabricated.

Four-point electrical measurements were made by applying different volt-ages (V) and measuring the resulting currents (I) flowing through

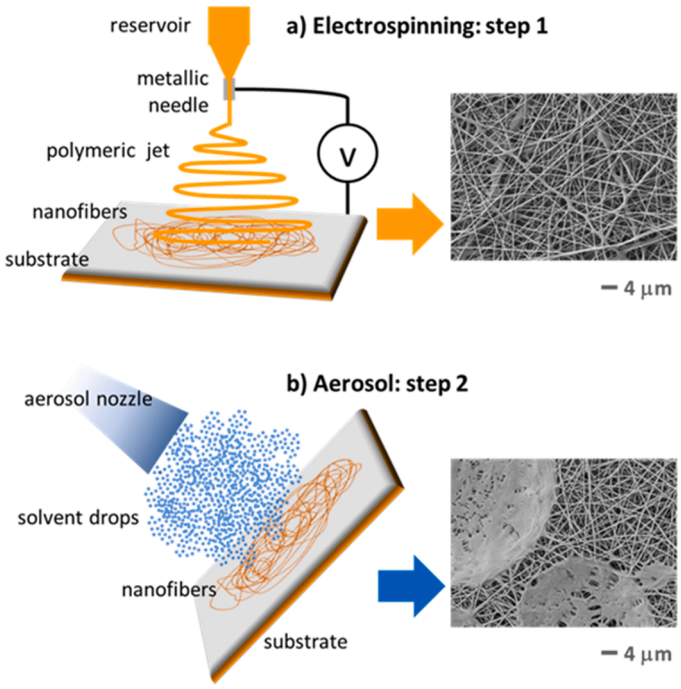

Fig. 1. Sketch of the AMLD process. It is made of two steps: in a) the first one corresponds to a standard nanofibers mat deposition by electrospinning; in b) the second step is shown: it is based on the exposure of the as-electrospun to solvents drops obtained by aerosol atomization.

the sample by means of a Keithley 2635A Source measure unit.

2.3. Fabrication of the sensors and their characterization

PDMS sheets (Sylgard 184 by Dow Corning) were prepared as the flexible substrates for the sensors, using a 10:1 weight ratio of PDMS to crosslinking agent. The crosslinking step was performed at 75°C for 3 h in oven. The molds were made of PMMA by CNC milling machine in such a way to obtain PDMS substrates 5 cm long, 3 cm wide and 2 mm thick. Electrodes were fabricated on the substrates using a composite flexible material obtained by mixing PDMS (standard 10:1 ratio) with 10 wt% MWCNT. [49] The PDMS/MWCNTs mixture was spread on the flexible substrate to create 2 electrodes for electrical characterizations at a distance of 2 cm and cured at 150°C for 1h.

Microporous mats of composite nanofibers were deposited directly onto the flexible PDMS substrates using a rigid PMMA hard mask fabricated with a CNC milling machine to obtain 1.75-cm-wide sensing strips. The parameters used for the electrospinning process were the same described in the previous paragraph.

To simulate the behavior of human body joints, such knees and elbows, piezoresistive analysis was performed by inducing deformation of flex-sensors in bending mode. Samples were mounted on the joint of a mechanical arm. Positioning was facilitated by the sticky behavior of PDMS surfaces and enhanced with a side clamp. Alligator clips were used to contact the PDMS/MWCNTs electrodes, avoiding stress to the sensitive NFs. Tests were performed changing the bending angle from 15° to 60°, inducing principal compression in the microporous NF mats, measuring the electrical resistance R of the sensors. The dimensionless parameter $\Delta R/R_0$ was then calculated as the ratio of the change in the electrical resistance of the deformed sensor (R_t) to the undeformed one (R_0) over R_0. The Gauge Factor was obtained through the model described by Saggio et al. [50].

The sensors were used to monitor the motion of human elbow. To perform that analysis the sensors were placed on the inside part of the arm, in correspondence of the elbow. The sensor was blocked using

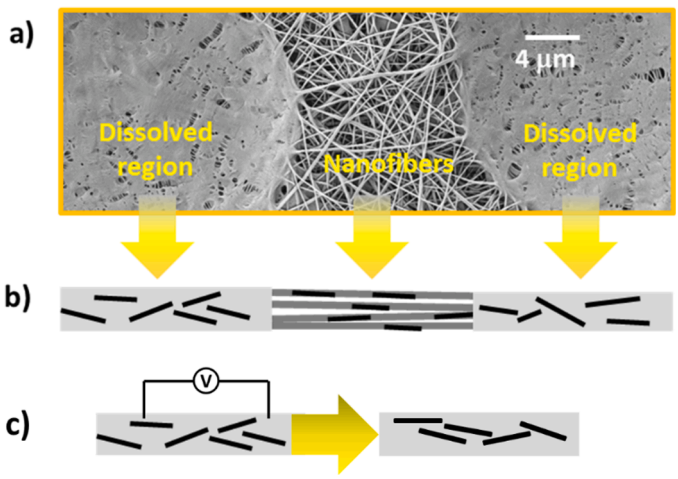

Fig. 2. The hybrid structure obtained by AMLD with and without of voltage application is shown in a) in b) its simplified representation is proposed and in c) scheme proposed the effect of voltage onto MWCNTs placed into the drop obtained by aerosol.

electrically insulating and flexible adhesive tape. During the arm movement, the current through the sensor was measured using a Keithley 2635A Source Meter.

3. Results and discussion

3.1. AMLD process description and characterization

The AMLD process is based on two steps, as depicted in Fig. 1. The first step consists of fabricating the nanofibers of interest by solution-based electrospinning (Fig. 1a)). The electrospinning step is performed by applying a voltage difference between a needle and a counter electrode on which nanofibers are collected. In this work, PEO/MWCNTs composite nanofibers were fabricated starting from an aqueous solution in which a variable loading of PSS-functionalized MWCNTs, from 1 to 7 wt%, was used. The use of PEO with a high molecular weight of 1000 kDa for the preparation of the composite nanofibers containing MWCNTs allowed us to obtain nanofiber mats with a dense hierarchical nanofiber netting structure already described in our previous work Massaglia et al. [44] In that study it is shown that the number of nanofiber nets increases with the concentration of MWCNTs and with the voltage applied during the electrospinning process.

After electrospinning the nanofiber mats were exposed to solvent droplets obtained by aerosol. The solvent droplets induced the local dissolution that characterizes the AMLD process (Fig. 1b)). When the water-based droplets hit the nanofiber mats, they locally induced dissolution of nanofibers promoting bonds among those NFs placed in the treated regions only. Importantly, the microporous nanofiber mat changed its structure only in the dissolved regions, while in the rest of the mat the nanofibers do not change their morphology, preserving their as-spun arrangement. This is particularly evident by comparing the FESEM images proposed in Fig. 1.

The AMLD process induces reorganization of the PEO/MWCNTs composite nanofibers due to the local dissolution of the polymer matrix of the nanofibers, as shown by the FESEM image in Fig. 2a). In the unmodified nanofibers the position of MWCNTs is that which characterizes the electrospinning process, as discussed in our previous paper from Massaglia et al. [44]. Indeed, as sketched in Fig. 2b), electrospinning induces strong alignment of CNTs in the main direction of the NFs. At the same time, the unmodified regions provide a true 3D microporous NF mat that can exhibit the best mechanical response to applied stress. Due to these features, the unmodified regions help to determine the final high sensitivity of the flex-sensor, while in the dissolved regions the

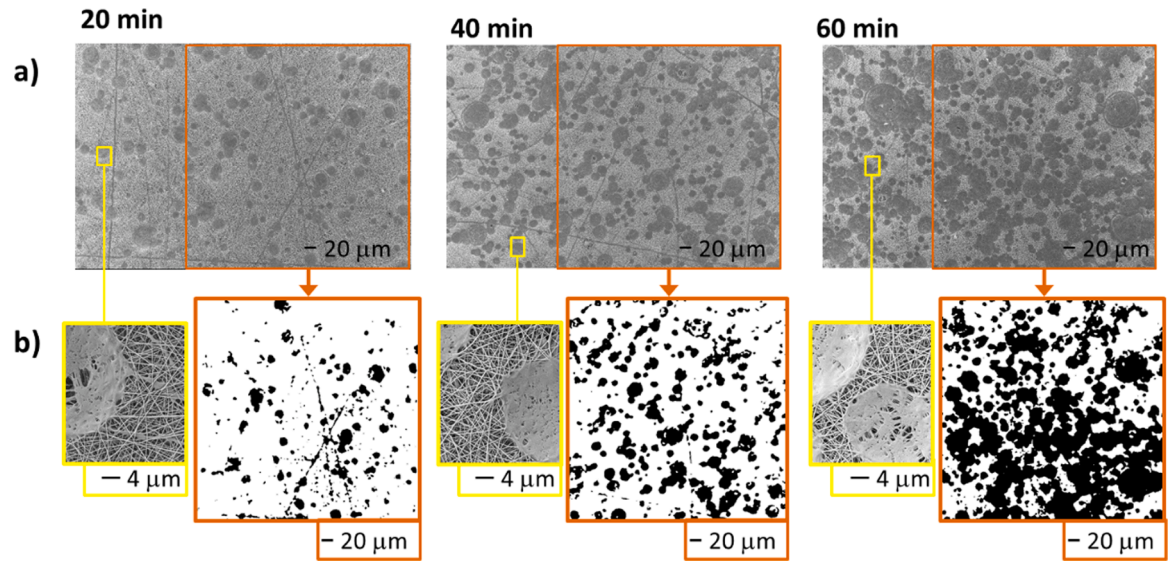

Fig. 3. In a) the morphology of PEO/MWCNTs nanofibers treated by AMLD process is proposed for different times, i.e. 20, 40 or 60 minutes. In b) enlargements of the treated regions are proposed highlighted in yellow, while the image analysis is highlighted in orange.

polymer matrix loses its nanostructured morphology, transforming into a denser structure (see Fig. 2a)) in which MWCNTs can easily create new and effective percolation pathways during the deformation process, locally improving the electrical conductivity. The overall arrangement resulting by AMLD processing is a 3D microporous NF hybrid mat.

In addition, since MWCNTs can reorganize into polymer matrices by application of a potential difference [47,48], we tested the effect of applying voltage during the AMLD process (V-AMLD), with the aim to promoting further improvement of the percolation threshold in the dissolved region, as depicted in Fig. 2c) [48].

The morphology of PEO/MWCNTs mats treated by AMLD at different processing times, i.e., 20, 40 and 60 minutes, was analyzed in detail by performing FESEM characterizations. The results are reported in Fig. 3, starting with the general overviews of the samples in Fig. 3a), which allow us to appreciate how the number of dissolved regions in the polymeric matrix increases progressively with exposure time, from 20 min to 60 min. Fig. 3b) highlights the regions where the hybrid structure is visible in the treated mats, alternating among dissolved and unmodified regions. Fig. 3b) allows to appreciate that during the AMLD process all the treated regions have similar morphologies regardless of processing time, what changes is the number of the dissolved regions after the process. This was demonstrated by processing the FESEM images with the aim to emphasize the contrast among light (unprocessed) and dark (dissolved) regions for the different processing times. The results are highlighted in orange in Fig. 3b): they demonstrate that AMLD is an effective approach to achieve control over the morphology of the 3D microporous NF mats transforming them into a controllable hybrid structure.

The electrical behavior of 3D microporous NFs was then analyzed. The samples were prepared by electrospinning as described in the previous section, with weight percentages of functionalized MWCNTs ranging from 1 to 7 wt%. For each composition, the performance of NF mats as obtained by electrospinning was compared to that of NFs treated by AMLD process at the three process times (20, 40 and 60 min). Finally,

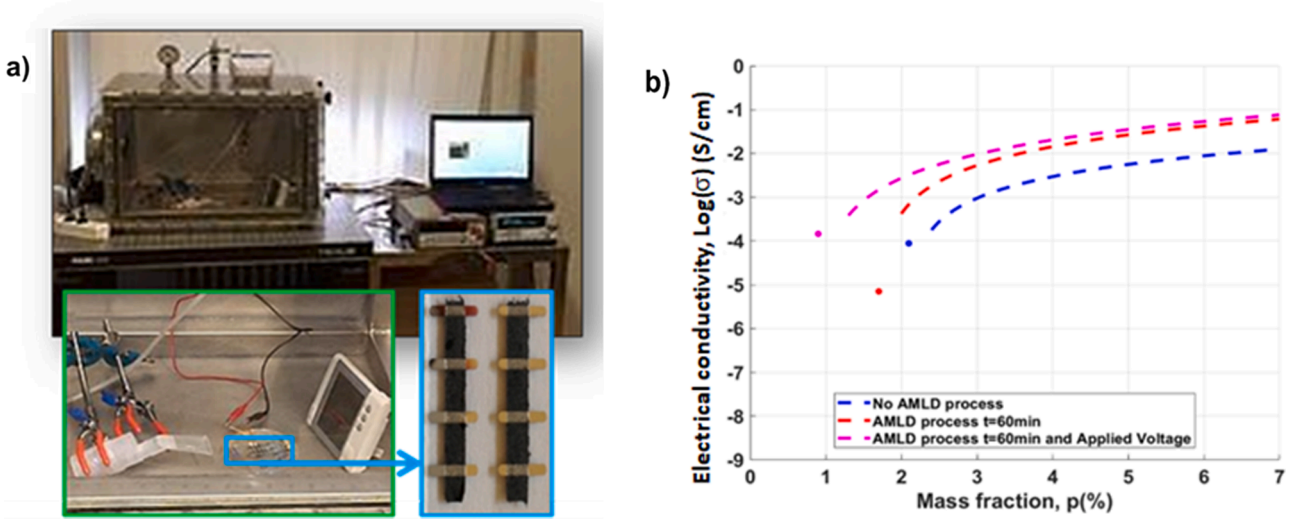

Fig. 4. In a) picture depicted the experimental setup to ensure AMLD process and AMLD process when an applied potential was applied, and the general structure of a sample is also proposed, showing Au electrodes sputtered on the nanofiber strip, in b) experimental values of the electrical conductivity of composite nanofibers PEO/MWCNTs without any treatment (blue line), composite nanofibers treated with AMLD process (red line) and composite nanofibers treated with AMLD process and an applied potential (purple line); the corresponding percolation thresholds are reported.

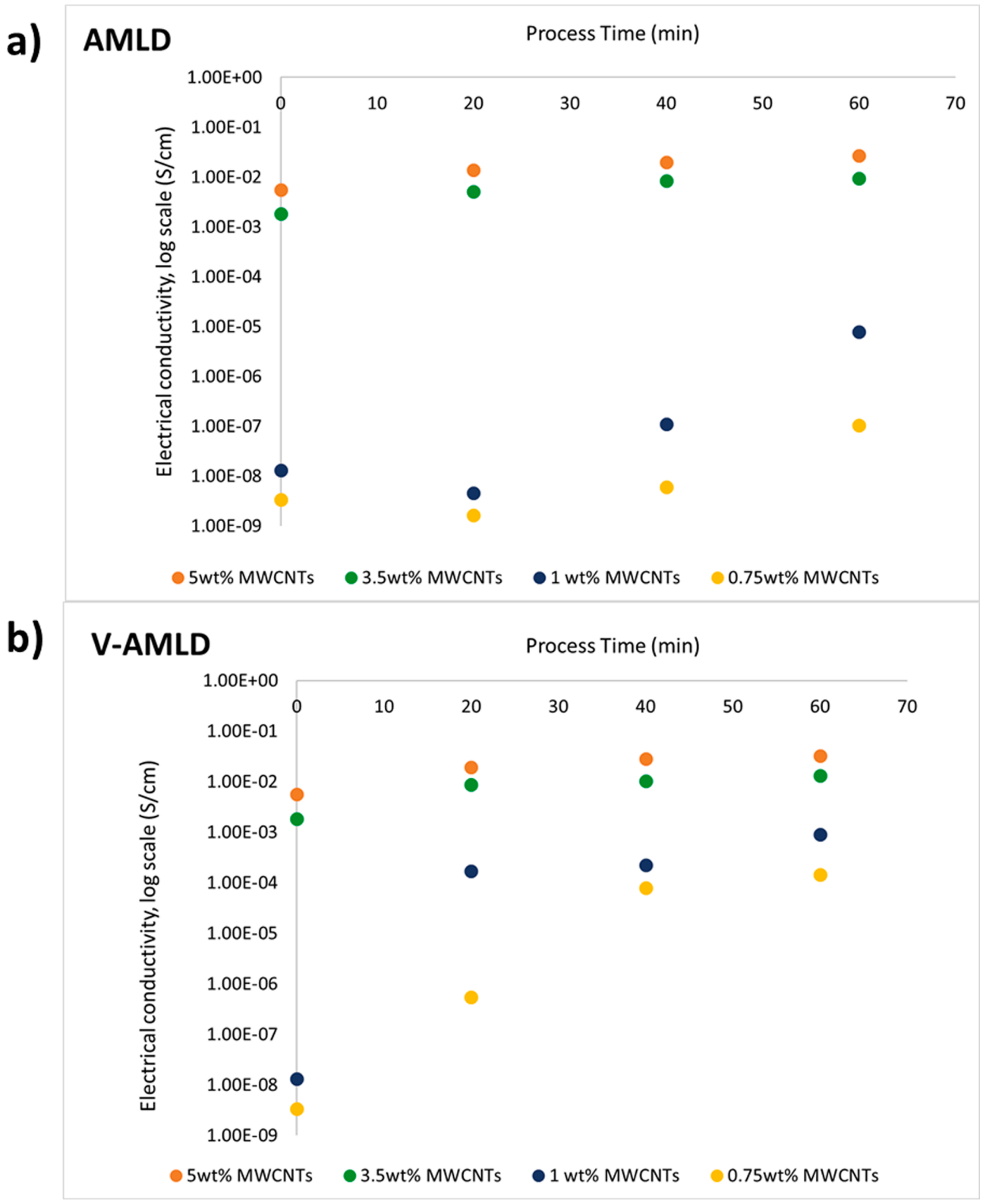

Fig. 5. In a) Electrical conductivity of composite nanofibers containing 0.75, 1, 3 and 5 wt% of MWCNTs treated with AMLD process, in b) Electrical conductivity of composite nanofibers with the same compositions but treated by V-AMLD process.

a third group of samples was fabricated and treated with V-AMLD, that is, with a 1 V applied voltage difference. Again, samples were fabricated with the different concentrations of MWCNT and using different AMLD treatment times. Based on previous work [44], we analyzed the data obtained for electrical characterization using the percolation models given in Eq.1 and Eq.2. The two equations describe the close correlation between the electrical conductivity of the final NF nanocomposite mat and the amount of MWCNTs above and below the percolation threshold, respectively:

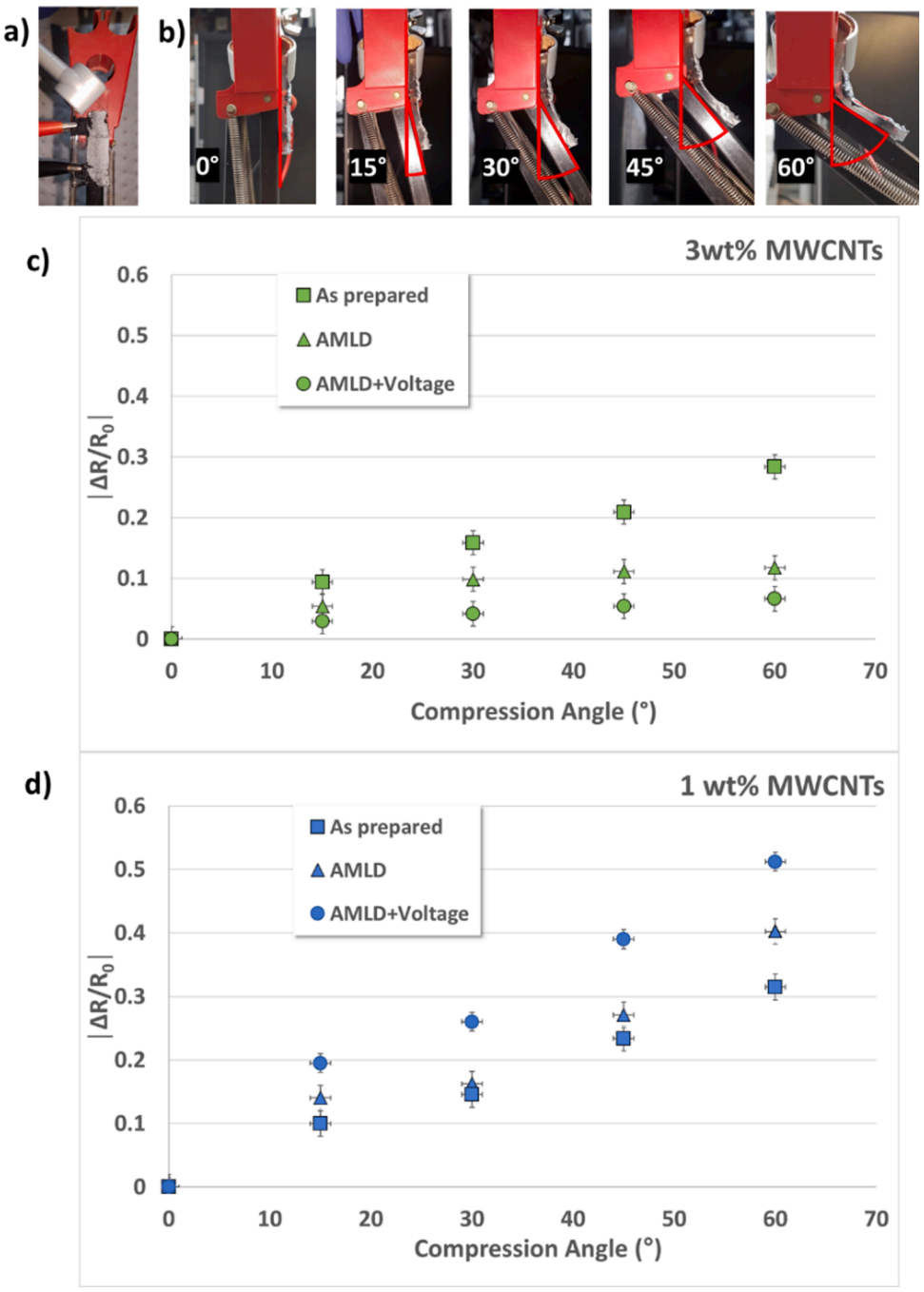

Fig. 6. In a) the sample mounted on the joint of the mechanical arm is shown before starting the bending characterization; in b) samples are proposed at different bending angles from 0° to 60°, in c) and d) piezoresistive characterizations of flexible sensors with nanostructured hybrid mats with 3 wt% and 1 wt% MWCNT are shown, respectively.

$$\sigma = \sigma_0 (p - p_c)^s \quad (1)$$

$$\sigma = \sigma_d (p_c - p)^t \quad (2)$$

In the percolation model, p_c is the percolation threshold, σ is the electrical conductivity, p is the weight percentage of MWCNTs and σ_0, σ_d,s, t are fit parameters.

The experimental setup used to study the AMLD process is shown in Fig. 4a), a closed and controlled chamber was used to treat the composite nanofibers with solvent droplets. A voltage generator and a multimeter were placed near the chamber and connected directly to a computer. To perform the electrical characterization, samples were fabricated using glass as the substrate. The overall structure of a sample is proposed in Fig. 4a), which also shows the Au electrodes sputtered on the nanofiber strip as electrical contacts.

The fit curves related to models of Eqs. 1 and 2 are proposed in Fig. 4b) for samples prepared by electrospinning only (blue curve), for NF mats treated by the AMLD process for 60 minutes (red curve), and for NF mats processed for 60 minutes plus the voltage difference (pink curve). The obtained values of the percolation thresholds are marked in the same figure by dots with the same colour of the corresponding curve. The electrical characterization of samples processed by ALMD and V-AMLD for 20 and 40 minutes are reported in the Supporting Information in Fig. S1 a) and b), respectively.

When AMLD process is applied, the observed percolation threshold is

1.7 wt% for all the processing times, showing that increasing the duration of the AMLD treatments have no significant effects of the electrical behavior of the sensors. Anyway, it is important to stress that with 20 minutes, the obtained value is lower than that obtained for untreated composite nanofibers, characterized by p_c value of 2.1 wt%. Samples processed by V-AMLD behave differently than those treated by AMLD. Samples treated for 40 minutes behave better than samples treated for 20 minutes only, with percolation thresholds pc that are equal to 1.5 and 1.1 wt%, respectively. As described in the main manuscript, the minimum p_c value of 0.9 wt% is found for samples prepared by 60 minutes long V-AMLD process.

The resulting hybrid structure in the nanofiber mat after the AMLD is particularly effective in improving accessibility of MWCNTs the one to the other, significantly facilitating the creation of a percolation pathway in the nanocomposite mats and thus increasing the electrical conductivity. The improvement is particularly high for samples with low MWCNTs loading. The obtained results make it possible to demonstrate that the modified regions created by AMLD process inducing the dissolution of the nanofibers, is effective to promoting tunneling phenomena among the MWCNTs in those regions. As a consequence, the percolation threshold value of the final 3D microporous NF hybrid mat is lower than that of the unprocessed nanofiber mat. Thus, this result allows us to demonstrate that the creation of controlled and localized connections among nanofibers in droplet-size regions is a key strategy to improve the electrical conductivity in this class of nanocomposites. Finally, it is very important to point out that the application of an electrical voltage of 1V during the AMLD process helps to further reduce the value of the percolation threshold, also increasing the electrical conductivity of nanofibers nanocomposite for all concentrations of MWCNTs. Indeed, the arrangement of MWCNTs in these regions obeys the field direction, so it is expected that the conductive continuous pathway is formed at a lower percolation threshold.

To better appreciate the characteristics of the AMLD and V-AMLD processes, Fig. 5 analyzes the effect of these two treatments on the electrical conductivity of PEO/MWCNTs nanofibers prepared with MWCNTs concentrations of 0.75 wt%, 1 wt%, 3 wt% and 5 wt%.

The AMLD process is analyzed in Fig. 5a). For untreated samples, the electrical conductivity of samples with 0.75 wt% and 1 wt% of MWCNTs is more than five orders of magnitude lower than that of samples with 1.5 wt% and 3 wt% of filler. Increasing the AMLD processing time the electrical conductivity of the nanocomposite material exhibits a slight increase. This is due to fact that the longer the time, the higher the number of droplets of solvent impinging the mat, and thus the higher the number of dissolved regions in which accessibility of MWCNTs is improved. Nevertheless, the improvement is not sufficient to further reduce the percolation threshold.

The results obtained for the V-AMLD process are reported in Fig. 5b). In this case, the effect of the external voltage is very effective in inducing a dramatic improvement of the electrical conductivity even for low processing time. The observed behavior can be explained by the effectiveness of the voltage difference in promoting the rearrangement of MWCNTs in locally dissolved areas, forcing them to adapt to the applied electric field. As explained above, during AMLD, polymeric NFs dissolve due to the effect of solvent droplets. The dissolution of adjacent NFs allows the creation of densely packed polymeric regions, and due to the applied tension the MWCNTs are mobile enough to rearrange themselves in the matrix before solvent evaporation, thus further improving the percolation pathway while increasing the processing time. The minimum value of the percolation threshold is obtained for a processing time of 60 minutes.

Thus, the results obtained allow us to confirm that the porosity, which characterizes nanofiber mats fabricated by electrospinning, significantly limits the properties of the resulting mats. Porosity is usually associated with the presence of an open structure between NFs, i.e., characterized by a low degree of connection among nanofibers. This work demonstrates that the controllable reduction of porosity, through the formation of junctions among the nanofibers, achieved through the AMLD process, proved to be crucial in ensuring an electrical conductivity enhancement of PEO/MWCNT composites nanofibers. The right balance between large surface area and large number of inter-fibers connections played a key role in defining the final properties of the 3D microporous NF hybrid mats. In addition, due to the local dissolution, the mobility of MWCNTs in the newly dissolved regions was sufficiently high to achieve further improvement in electrical conductivity through the application of an electrical potential difference during the V-AMLD process. The results obtained thus demonstrated the effectiveness of the potential applied during AMLD to achieve a higher electrical conductivity and a lower percolation threshold value.

Given such promising results obtained in terms of electrical behavior of the 3D microporous NF hybrid mats, they were integrated into flexible sensors.

3.2. *Flex sensors with hybrid nanostructured mats by AMLD process*

Flex sensors were fabricated with composite PEO/MWCNTs composite nanofibers deposited directly onto flexible PDMS substrates, with electrodes made of conductive PDMS/MWCNTs. PDMS was selected since it offers an optimal combination of skin compatibility, mechanical flexibility and electrical insulating properties, which are essential for the design of wearable sensors. The objective of this part of the work is to the verify the possibility of using the flex sensor to analyze the behavior of human body joints, such as knees and elbows. To achieve this goal, samples were mounted on the joint of a mechanical arm as shown in Fig. 6a), where the sample is also shown. The samples were secured through to the sticky behavior of PDMS surfaces and further enhanced with a side clamp; the optimal adherence can be appreciated from the side view of the setup in Fig. 6b). Piezoresistive analyses were performed by deforming the flex-sensors in bending mode, causing the nanofiber mats to deform especially in compression. [46] Different stress values were applied corresponding to the bending angles of 0°, 15°, 30° and 60°, as shown in Fig. 6b). For each value of the bending angle, the electrical resistance R of the sensitive hybrid nanostructured mats was measured. Starting from all results obtained in the previous part of this work regarding the electrical characterizations of the nanomaterials. Since nanocomposite materials with a MWCNTs concentration close to the percolation threshold are expected to have the best piezoresistive behavior, [51] we decided to perform the piezoresistive analysis by comparing the behavior of nanostructured hybrid mats with 1 wt% of MWCNTs with that of samples with 3 wt% of filler in order to compare the sensing behavior of samples below and above the percolation threshold, respectively. The 1 wt% of MWCNTs is close to the percolation also for samples treated by V-AMLD for 20 minutes, so that 20 min has been selected as the processing time also for the AMLD treatment. The results of the so performed analyses are described in Fig. 6c) and in d), for samples with 3 wt% MWCNTS and with a 1 wt% MWCNTS loading, respectively. In both figures, the dimensionless parameter $|\Delta R/R_0|$was calculated and plotted as a function of the compression angle. $|\Delta R/R_0|$ is the ratio of the change in the electrical resistance of the deformed sensor (R_t) with respect to the undeformed one (R_0) over R_0. For each composition, samples with sensitive layer formed by NFs prepared by electrospinning were compared with samples in which the sensitive nanofibers were also treated with AMLD and with V-AMLD.

All set of data show a linear trend of $|\Delta R/R_0|$ versus the bending angle, no matter the composition of the sensitive layer in term of MWCNTs concentration. Moreover, the samples with sensitive layers made of untreated electrospun NFs (i.e., as prepared) show no significant difference of the values of $|\Delta R/R_0|$ versus the bending angle no matter the composition.

The behavior observed for samples with 1 and 3 wt% MWCNTs is completely different when they are processed with the AMLD and V-AMLD treatments. In particular, Fig. 6d) shows that for samples prepared with 1 wt% of MWCNTs the value of $|\Delta R/R_0|$ for each angle is

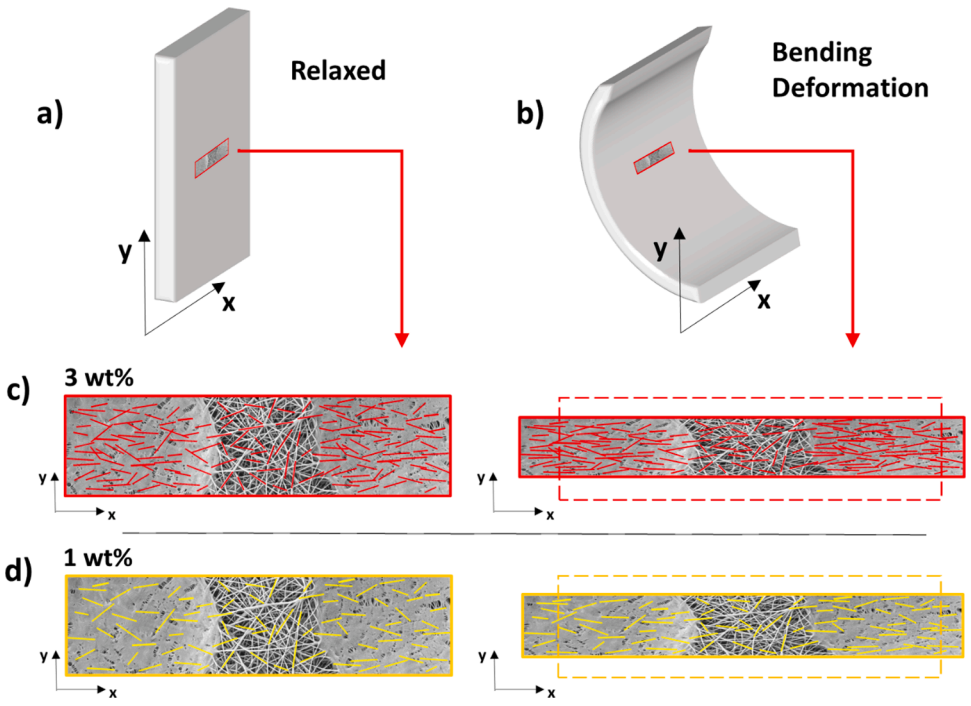

Fig. 7. In a) the relaxed sample in sketched. In b) the same sample is sketched during bending. A central portion of the sample is made evident in both a) and b), characterized of two dissolved regions connected by an unmodified NF mat. In c) pictures of the central part are proposed in red color to represent the 3 wt% of MWCNTs. In d) yellow is used to depict the 1 wt % loading. In both c) and d) the left side shows the undeformed central region, while on the roght the region is prone to deformation.

higher for samples treated by AMLD and V-AMLD, with the best sensitivity for V-AMLD treated samples. This behavior is consistent to the ability of the newly developed NF microporous 3D hybrid mats to offer higher changes of the electrical conductivity for large applied stress, indeed for low filler concentration the application of compressive mode stresses increases the probability of building new conductive paths along the direction of the applied stress. [3] V-AMLD treatment improves the alignment of MWCNTs within nanocomposite strain sensors; this has been shown to make the tunnelling resistance more responsive to strain, with a dramatic increase in sensitivity. [52] The trend is opposite for for samples at 3 wt%, where AMLD and V-AMLD processes have negative effects on the piezoresistive behavior of the hybrid nanostructured mats, as shown in Fig. 6c). To explain the observed behavior, it is important to consider that samples with 3 wt% of MWCNTs are well above the percolation threshold, and thus characterized by a very good electrical behavior, and AMLD and V-AMLD have no effect on samples, as shown in Fig. 5. In samples with such high loading the main effect of both AMLD and V-AMLD is to change the morphology of the samples, creating microscale dissolved regions in which the polymer is no longer nanostructured. Such dissolved regions react to the bending stress as a whole, while nanofibers respond mainly individually and a collective response arise only because of the entanglements among them. The morhology of the samples and a sketch of the effect of deformation on them is proposed in Fig. 7a) and b).

This different mechanical response explains the observed opposite trend in the piezoresistive behavior of samples above and below the percolation threshold. Indeed, when samples with high MWCNTs loading are bended (see Fig. 7c) right side), the deformation of the dissolved regions induces a more direct contact among MWCNTs, improving charge transfer. A similar behavior characterizes the unmodified NF-based regions. Nevertheless, at the interface among dissolved and unmodified regions the applied stress is less effective, being prone to a transition of the material between a nanostructured area and a sort of bulky state. For high loading of conductive filler this has a detrimental effect on the tunneling phenomena among dissolved regions and adjacent unmodified NFs, reducing the electrical conductivity. When samples with 1 wt% of MWCNTs are tested, the opposite trend is observed. As shown in Fig. 7 d) the application of stress in this kind of samples is always very effective in increasing the probability of building new conductive paths among MWCNTs along the direction of the applied stress. The improvement occurs in both the two regions and among them. Morphology has a key role in the mechanism proposed so far in Fig. 7. Nanostructured hybrid mats with a high concentration of filler, experience severe damage to the overall conductive pathways of MWCNTs when they are treated by AMLD. This is due to the transition among dense and porous (i.e. nanostructured) matrix along the stress direction. Indeed, the creation of densely packed regions by AMLD enhances the destruction effect of applied stress, and the application of voltage during AMLD promote further changes of the MWCNTs conductive network that are detrimental for the overall response of the sensor [3].

Finally, the Gauge Factor (GF) of the flex sensors was analysed. The calculation is based on the following model [46]:

$$GF = \frac{\Delta R}{R_0}\cdot\frac{1}{\Delta\varphi}\cdot\frac{2l_{tot}}{h}$$

Where $\Delta\varphi$ is the angular strain expressed in radians and it is associated with the compression angles shown in Fig. 6b), l_{tot} is the length of the sensitive 3D microporous NF mat, and h is the thickness of the PDMS substrate. The resulting GF values are shown in Fig. 8a) for both the samples with 1 wt% MWCNT and 3 wt% MWCNT.

The GF value obtained for flex sensors having NFs prepared by electrospinning only as the sensitive layer is equal to 296.6 and 322.8 for samples at 3 wt% MWCNTs and 1 wt% MWCNTs, respectively. These results compare very well with the data we obtained in our previous work [46] and more generally with the literature [53,54]. Interestingly, the GF value is higher for devices with lower filler content. This funding is in line with the results proposed by Garcia et al. [55], who demonstrate a strong dependence of the gauge factor on the filler concentration in nanocomposite strain sensors. More specifically, the gauge factor diverges as the volume fraction of filler approaches the percolation threshold, with a decrease of its value as filler loading increases. For each composition, GFs of flex sensors with NFs prepared only by electrospinning are compared with the GFs of flexible sensors obtained with sensitive NFs treated by AMLD and V-AMLD. Similar to what was observed for the piezoresistive characterization described in Fig. 6, the

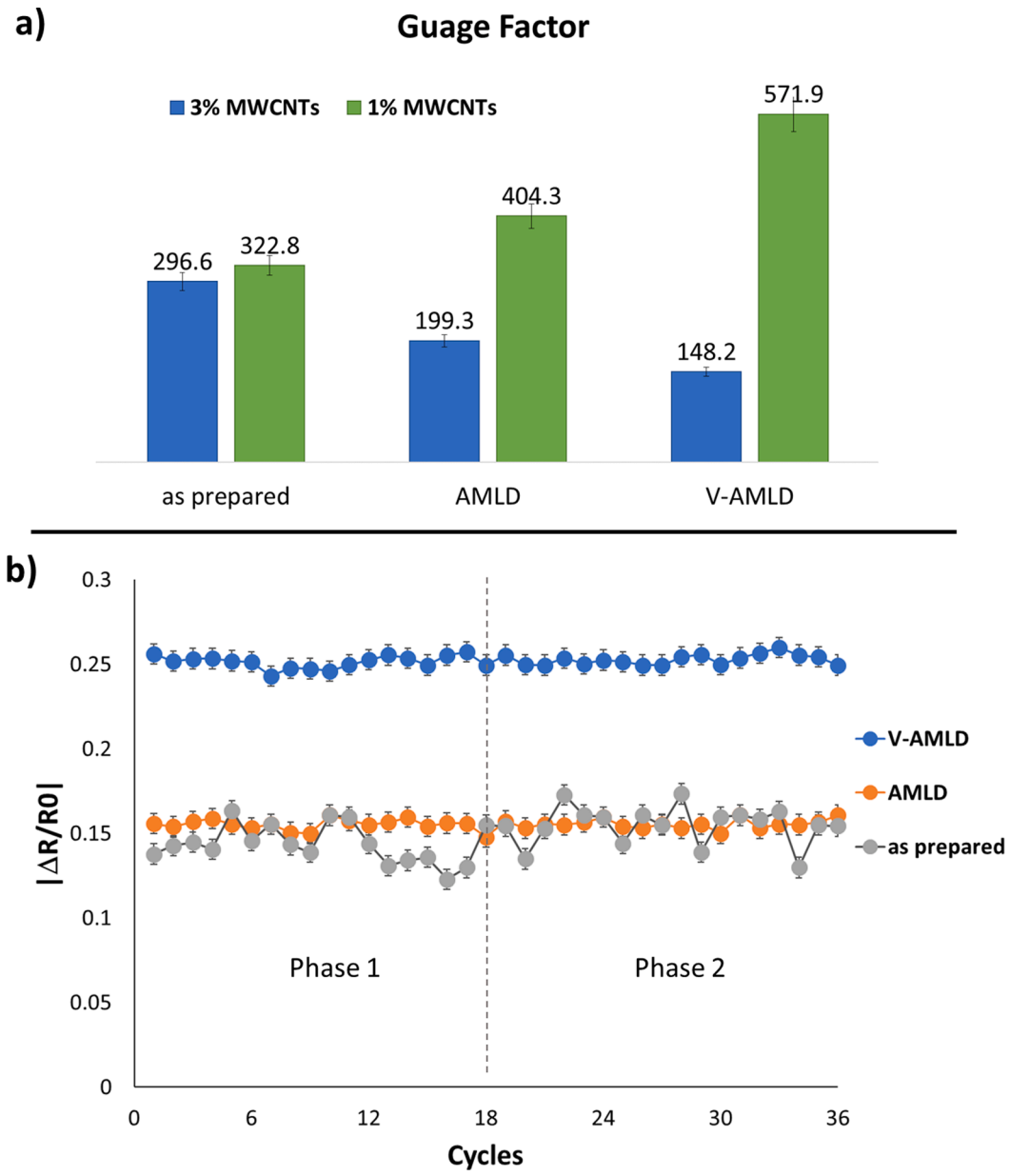

Fig. 8. In a) Gauge Factors of flex sensors with nanostructured mats containing 3 wt% MWCNTs are compared to GFs of sensors prepared using mats with 1 wt% MWCNTs. AMLD and V-AMLD processed have been tested on each class of 3D nanocomposite materials. In b) the stability over time is analysed for all the type of sensors with 1 wt% of MWCNTs and a deformation angle of 30°.

GFs have opposite trends for samples with 3 wt% MWCNTs and 1 wt% MWCNTs. For low filler content, both AMLD and V-AMLD contribute significantly to further improve the sensitivity of the sensor, reaching an outstanding value of 571.9. The behaviour of samples with 3 wt% MWCNTs is opposite, with a further decrease in GF of the devices whose nanostructured sensing layer was treated with AMLD and V-AMLD. The results to date demonstrate the great potential of AMLD and V-AMLD to design and fabricate wearable flex sensors with a dramatic reduction in MWCNTs loading, expanding the application potential of this class of sensors.

The stability and reliability of the sensors were analysed by repeating bending and release cycles. Tests were conducted at a deformation angle of 30° on the sensors with 1 wt% MWCNTs either directly prepared by electrospinning or treated by AMLD and V-AMLD processes for 20 min. During each test, i.e. cycle, the sensor was bended and released for 20 consecutive times. In the supporting information, Fig. S2 shows the setup used to performed the stability, while Fig. S3 shows the data of current versus time referring to 4 consecutive repetitions. Starting from the values of the current as a function of time, the average value of the $|\Delta R/R_0|$ parameter for each test (i.e., a cycle) of 20 repetitions was calculated. The values of $|\Delta R/R_0|$ for each cycle are shown in Fig. 8(b). The results show good stability for sensors from electrospinning and excellent behaviour for sensors processed with both AMLD and V-AMLD. A supporting video is available, showing part of a stability cycle. The points reported in Fig. 8b) were acquired in two separate phases: the first phase includes the first 18 test cycles and refers to measurements conducted over 3 months; the second phase refers to the last 18 test cycles conducted on the same sensors after a break of 3 months later and refers to measurements conducted over 2 months. During the period between the 2 phases, the sensors were stored in laboratory cabinets. The long-term tests conducted revealed excellent stability and reliability for the AMLD and V-AMLD sensors.

Finally, the flexible sensor with 1 wt% MWCNT treated by V-AMLD process for 20 minutes has been tested in real-time for human body

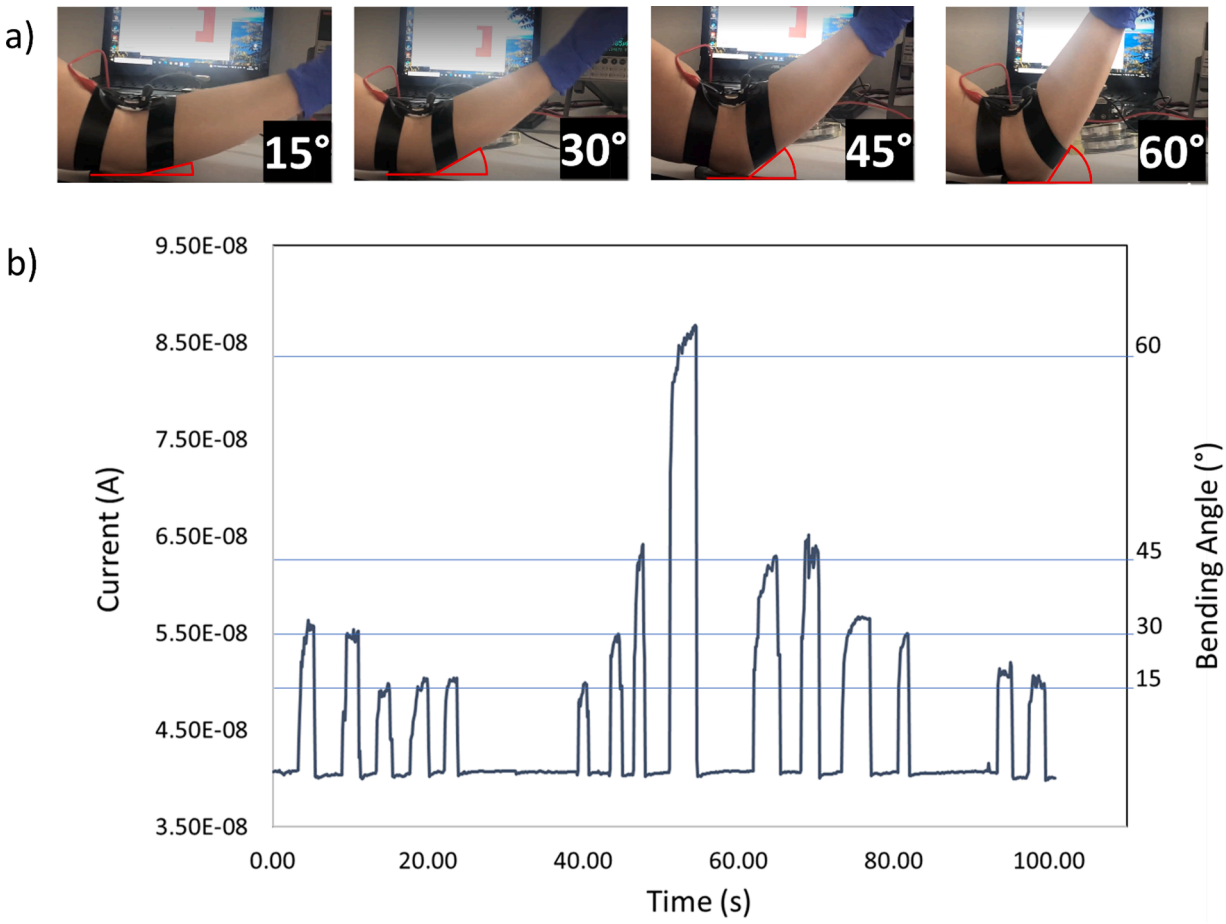

Fig. 9. Test on human body for real time elbow monitoring: in a) pictures show the position of arm during the measurements, in b) the real time results in terms of current change during flexion of the sensor are reported.

activity monitoring. To carry out the test, the sensor was placed on the inside of the arm, at the elbow, as shown in Fig. 9a). The arm was moved continuously to cause bending of the sensor, and the corresponding current changes through sensor was recorded. For each angle value tested with the mechanical arm, i.e. 15°, 30°, 45°, and 60°, the human arm was held still to record the peak current value for that angle and then returned to a horizontal (rest) position. The setup used for real time tests is described in the supporting information (see Fig. S4) and a supporting video shows a real time measurement. In Fig. 9b) the current peaks recorded during real time elbow monitoring are reported and associated to the corresponding angle. The values obtained are in line with those observed during the tests conducted with the mechanical arm."

4. Conclusions

In the present work, the AMLD process to fabricate a 3D microporous hybrid NF mat from PEO/MWCNTs composite nanofibers by electrospinning is reported. The nanostructured composite materials have been shown to exhibit a higher electrical conductivity than NF mat from PEO/MWCNTs prepared only by electrospinning. The improvement is particularly high for samples with low MWCNT content, even below the original percolation threshold, due to the improved percolation pathway achieved by increasing the connections between. The improved electrical conductivity is accompanied by exceptional sensitivity of the flexible sensor for low MWCNT contents. This is due in particular to the ability of the AMLD process to preserve the high surface area of the 3D mat, inducing improved fiber-to-fibers contacts only in certain regions. Finally, this work shows that further improvement can be achieved by inducing the alignment of MWCNTs during the AMLD process applying a potential difference. The combination of voltage and local dissolution allows exploiting the mobility of MWCNTs in the regions that are being dissolved, resulting in a marked improvement in GF (571.9) for sensors with a MWCNT loading of only 1 wt%. These results help further expand the applicability of flexible sensors in wearable and healthcare applications.

Author contributions

The authors equally contributed to the work based on their different academic roles.

CRediT authorship contribution statement

Marzia Quaglio: Conceptualization, Investigation, Validation, Resources, Writing – review & editing, Supervision, Project administration. **Candido F. Pirri:** Funding acquisition. **Giulia Massaglia:** Conceptualization, Investigation, Validation, Resources.

Declaration of Competing Interest

The authors declare that they have no known competing financial interests or personal relationships that could have appeared to influence the work reported in this paper

Data availability

Data will be made available on request.

Funding

This study was partially carried out within the MICS (Made in Italy – Circular and Sustainable) Extended Partnership and received funding from the European Union Next-GenerationEU (PIANO NAZIONALE DI RIPRESA E RESILIENZA (PNRR) – MISSIONE 4 COMPONENTE 2, INVESTIMENTO 1.3 – D.D. 1551.11-10-2022, PE00000004). This manuscript reflects only the authors' views and opinions, neither the European Union nor the European Commission can be considered responsible for them.

Supplementary materials

Supplementary material associated with this article can be found, in the online version, at doi:10.1016/j.apmt.2023.101863.

References

[1] J. Yoo, D-Y. Kim, H. Kim, O-N. Hur, S-H. Park, Comparison of pressure sensing properties of carbon nanotubes and carbon black polymer composites, Materials 15 (2022) 1213, https://doi.org/10.3390/ma15031213.
[2] L. Chen, G. Chen, L. Lu, "Piezoresistive behavior study on finger-sensing silicone rubber/graphite nanosheet nanocomposites", Adv. Funct. Mater. 17 (2007) https://doi.org/10.1002/adfm.200600519, 898–90.
[3] O. Kanoun, A. Bouhamed, R. Ramalingame, J.R. Bautista-Quijano, D. Rajendran, A. Al-Hamry, Review on conductive polymer/CNTs nanocomposites based flexible and stretchable strain and pressure sensors, Sensors 21 (2021) 341, https://doi.org/10.3390/s21020341.
[4] Y.-F. Chen, M.-L. Huang, J.-H. Cai, Y.-X. Weng, M. Wang, Piezoresistive anisotropy in conductive silicon rubber/multi-walled carbon nanotube/nickel particle composites via alignment of nickel particles, Composit. Sci. Technol. 225 (2022), 109520, https://doi.org/10.1016/j.compscitech.2022.109520.
[5] J.-H. Cai, J. Lia, X.-D. Chen, M. Wang, Multifunctional polydimethylsiloxane foam with multi-walled carbon nanotube and thermo-expandable microsphere for temperature sensing, microwave shielding and piezoresistive sensor, Chem. Eng. J. 393 (2020), 124805, https://doi.org/10.1016/j.cej.2020.124805.
[6] Y.-F. Chen, J. Li, Y.-J. Tan, J.-H. Cai, X.-H. Tang, J.-H. Liu, M. Wang, Achieving highly electrical conductivity and piezoresistive sensitivity in polydimethylsiloxane/multi-walled carbon nanotube composites via the incorporation of silicon dioxide micro-particles, Compos. Sci. Technol. 177 (2019) 41–48, https://doi.org/10.1016/j.compscitech.2019.04.017.
[7] B. Zazoum, K.M. Batoo, M.A.A. Khan, Recent advances in flexible sensors and their applications, Sensors 22 (2022) 4653, https://doi.org/10.3390/s22124653.
[8] J. Cai, M. Du, Z. Li, Flexible temperature sensors constructed with fiber materials, Adv. Mater. Technol. 7 (2022), 2101182, https://doi.org/10.1002/admt.202101182.
[9] Z. Pang, Y. Zhao, N. Luo, D. Chen 1, M. Chen, Highly sensitive piezoresistive pressure sensor based on super-elastic 3D buckling carbon nanofibers for human physiological signals' monitoring, Nanomaterials 12 (2022) 2522, https://doi.org/10.3390/nano12152522.
[10] Y. Gao, L. Yu, J.C. Yeo, C.T. Lim, Flexible hybrid sensors for health monitoring: materials and mechanisms to render wearability, Adv. Mater. 32 (2020), 1902133, https://doi.org/10.1002/adma.201902133.
[11] W. Schwalb, Y. Wang, Y. Chen, Y. Tang, J. Si, B. Shirinzadeh, W. Cheng, A wearable and highly sensitive pressure sensor with ultrathin gold nanowires, Nat. Commun. 5 (2014) 1–8, https://doi.org/10.1038/ncomms4132.
[12] D.J. Lipomi, M. Vosgueritchian, B.C.-K. Tee, S.L. Hellstrom, J.A. Lee, C.H. Fox, Z. Bao, Skin-like pressure and strain sensors based on transparent elastic films of carbon nanotubes, Nat. Nanotechnol. 6 (2011) 788–792, https://doi.org/10.1038/nnano.2011.184.
[13] H.B. Yao, J. Ge, C.F. Wang, X. Wang, W. Hu, Z.J. Zheng, A flexible and highly pressure-sensitive graphene-polyurethane sponge based on fractured microstructure design, Adv. Mater. 25 (2013) 6692–6698, https://doi.org/10.1002/adma.201303041.
[14] S. Zhao, G. Zhang, Y. Gao, L. Deng, J. Li, R. Sun, C.P. Wong, Strain-driven and ultrasensitive resistive sensor/switch based on conductive alginate/nitrogen-doped carbon-nanotube-supported Ag hybrid aerogels with pyramid design, ACS Appl. Mater. Interface. 6 (2014) 22823–22829, https://doi.org/10.1021/am5069936.
[15] J.W. Park, J. Jang, Fabrication of graphene/free-standing nanofibrillar PEDOT/P (VDF-HFP) hybrid device for wearable and sensitive electronic skin application, Carbon 87 (2016) 275–281, https://doi.org/10.1016/j.carbon.2015.02.039.
[16] C. Yan, J. Wang, W. Kang, M. Cui, X. Wang, C.Y. Foo, K.J. Chee, P.S. Lee, Highly stretchable piezoresistive graphene-nanocellulose nanopaper for strain sensors, Adv. Mater. 26 (2014) 2022–2027, https://doi.org/10.1002/adma.201304742.
[17] P. Pötschke, H. Brünig, A. Janke, D. Fischer, D. Jehnichen, Orientation of multiwalled carbon nanotubes in composites with polycarbonate by melt spinning, Polymer 46 (2005) 10355–10363, https://doi.org/10.1016/j.polymer.2005.07.106.
[18] P. Pötschke, T. Andres, T. Villmow, S. Pegel, H. Brünig, K. Kobashi, D. Fischer, L. Häussler, Liquid sensing properties of fibres prepared by melt spinning from poly (lactic acid) containing multi-walled carbon nanotubes, Compos. Sci. Technol. 70 (2010) 343–349, https://doi.org/10.1016/j.compscitech.2009.11.005.
[19] J.R. Bautista-Quijano, P. Pötschke, H. Brünig, G. Heinrich, Strain sensing, electrical and mechanical properties of polycarbonate/multiwall carbon nanotube monofilament fibers fabricated by melt spinning, Polymer 82 (2016) 181–189, https://doi.org/10.1016/j.polymer.2015.11.030.
[20] N. Wen, L. Zhang, D. Jiang, Zi. Wu, B. Li, C. Sun, Z. Guo, Emerging flexible sensors based on nanomaterials: Recent status and applications, J. Mater. Chem. A 8 (2020) 25499–25527, https://doi.org/10.1039/D0TA09556G.
[21] W. Yan, T. Yokota, T. Someya, Electrospun nanofiber-based soft electronics, NPG Asia Mater. 13 (2021) 1–22, https://doi.org/10.1038/s41427-020-00267-8.
[22] S. Cai, C. Xu, D. Jiang, M. Yuan, Q. Zhang, Z. Li, Y. Wang, Air-permeable electrode for highly sensitive and noninvasive glucose monitoring enabled by graphene fiber fabrics, Nano Energy 93 (2022), 106904, https://doi.org/10.1016/j.nanoen.2021.106904.
[23] J.Yu M.Zhu, Z. Li, B. Ding, Self-healing fibrous membranes, Angew. Chem. Inter. Ed. 61 (2022), https://doi.org/10.1002/anie.202208949 e202208949.
[24] B. Xue, H. Xie, J. Zhao, J. Zheng, C. Xu, Flexible piezoresistive pressure sensor based on electrospun rough polyurethane nanofibers film for human motion monitoring, Nanomaterials 12 (2022) 723, https://doi.org/10.3390/nano12040723.
[25] J.H. Wendorff, S. Agarwal, Andreas Greiner, Electrospinning: Materials, Processing, and Applications, Wiley-VCH Verlag GmbH & Co. KGaA, 2012.
[26] H.S. Yoo, T.G. Kim, T.G. Park, Surface-functionalized electrospun nanofibers for tissue engineering and drug delivery, Adv. Drug Deliv. Rev. 61 (2009) 1033–1042, https://doi.org/10.1016/j.addr.2009.07.007.
[27] F.E. Ahmed, B.S. Lalia, R. Hashaikeh, A review on electrospinning for membrane fabrication: Challenges and applications, Desalination 356 (2015) 15–30, https://doi.org/10.1016/j.desal.2014.09.033.
[28] S. Agarwal, A. Greiner, J.H. Wendorff, Functional materials by electrospinning of polymers, Progr. Polym. Sci. 38 (2013) 963–991, https://doi.org/10.1016/j.progpolymsci.2013.02.001.
[29] K. Mondal, A. Sharma, Recent advances in electrospun metal-oxide nanofiber based interfaces for electrochemical biosensing, RSC Adv. 6 (2016) 94595, https://doi.org/10.1039/C6RA21477K.
[30] D.H. Reneker, A-L Yarin, S.Koombhongse H, Bending instability of electrically charged liquid jets of polymer solutions in electrospinning, J. Appl. Phys. 87 (2000) 4531, https://doi.org/10.1063/1.373532.
[31] V. Thavasi, G. Singh, S. Ramakrishna, Electrospun nanofibers in energy and environmental applications, Energy Environ. Sci. 1 (2008) 205–221, https://doi.org/10.1039/B809074M.
[32] B. Ding, M. Wang, J. Yu, G. Sun, Gas sensors based on electrospun nanofibers, Sensors 9 (2009) 1609–1624, https://doi.org/10.3390/s90301609.
[33] Y. Dai, W. Liu, E. Formo, Y. Sun, Y. Xia, Ceramic nanofibers fabricated by electrospinning and their applications in catalysis, environmental science, and energy technology, Polym. Adv. Technol. 22 (2011) 326–338, https://doi.org/10.1002/pat.1839.
[34] G. Massaglia, M. Quaglio, Semiconducting nanofibers in photoelectrochemistry, Mater. Sci. Semicond. Process. 73 (2018) 13–21, https://doi.org/10.1016/j.mssp.2017.06.047.
[35] M. Zhu, J. Li, J. Yu, Z. Li, B. Ding, Superstable and intrinsically self-healing fibrous membrane with bionic confined protective structure for breathable electronic skin, Angew. Chem. Int. Ed. 61 (2022), https://doi.org/10.1002/anie.202200226 e202200226.
[36] A. Vitale, G. Massaglia, A. Chiodoni, R. Bongiovanni, C.F. Pirri, M. Quaglio, Tuning porosity and functionality of electrospun rubber nanofiber mats by photo-crosslinking, ACS Appl. Mater. Interface. 11 (27) (2019) 24544–24551, https://doi.org/10.1021/acsami.9b04599.
[37] P.-C. Lee, T.-H. Han, T. Hwang, J.-S. Oh, S.-J. Kim, B.-W. Kim, Y. Lee, H.R. Choi, S. K. Jeoung, S.E. Yoo, J.-D. Nam, Electrochemical double layer capacitor performance of electrospun polymer fiber-electrolyte membrane fabricated by solvent-assisted and thermally induced compression molding processes, J. Membr. Sci. 409–410 (2012) 365–370, https://doi.org/10.1016/j.memsci.2012.04.007.
[38] F.E. Ahmed, B.S. Lalia, R Hashaikeh, A review on electrospinning for membrane fabrication: challenges and applications, Desalination 356 (2015) 15–30, https://doi.org/10.1016/j.desal.2014.09.033.
[39] Y. Chen, N. Wang, M. Jensen, X. Li, Low-temperature welded PAN/TPU composite nanofiber membranes for water filtration, J. Water Process Eng. 47 (2022), 102806, https://doi.org/10.1016/j.jwpe.2022.102806.
[40] N.D. Luong, I.S. Moon, J.-D. Nam, A solvent-assisted compression molded of poly(l-lactide)/hydroxyapatite electrospun fibers for robust engineered scaffold systems, Macromol. Mater. Eng. 294 (2009) 699–704, https://doi.org/10.1002/mame.200900204.
[41] Y.H. Lee, J.H. Lee, I.-G. An, C. Kim, Y. Lee, J.-D. Nam, Electrospun dual-porosity structure and biodegradation morphology of Montmorillonite reinforced PLLA nanocomposite scaffolds, Biomaterials 26 (2005) 3165–3172, https://doi.org/10.1016/j.biomaterials.2004.08.018.
[42] S. Ramaswamy, L.I. Clarke, R.E. Gorga, Morphological, mechanical, and electrical properties as a function of thermal bonding in electrospun nanocomposites, Polymer 52 (2011) 3183–3189, https://doi.org/10.1016/j.polymer.2011.05.023.
[43] T. Xu, Y. Ding, Z. Wang, Y. Zhao, W. Wu, H. Fong, Z. Zhu, Three-dimensional and ultralight sponges with tunable conductivity assembled from electrospun nanofibers for a highly sensitive tactile pressure sensor, J. Mater. Chem. C 5 (2017) 10288, https://doi.org/10.1039/c7tc03456c.
[44] G. Massaglia, A. Chiodoni, G.P. Salvador, L. Delmondo, J.A. Muñoz-Tabares, S. Bocchini, A. Sacco, S. Bianco, G. Saracco, M. Quaglio, Defining the role of

nanonetting in the electrical behaviour of composite nanofiber/nets, RSC Adv. 7 (2017) 38812, https://doi.org/10.1039/C7RA05573K.
[45] E. Verpoorten, G. Massaglia, C.F. Pirri, M. Quaglio, Electrospun PEO/PEDOT:PSS nanofibers for wearable physiological flex sensors, Sensors 21 (12) (2021) 4110, https://doi.org/10.3390/s21124110.
[46] E. Verpoorten, G. Massaglia, G. Ciardelli, C.F. Pirri, M. Quaglio, Design and optimization of piezoresistive PEO/PEDOT:PSS electrospun nanofibers for wearable flex sensors, Nanomaterials 10 (11) (2020) 2166, https://doi.org/10.3390/nano10112166.
[47] P.S. Goh, A.F. Ismail, B.C. Ng, Directional alignment of carbon nanotubes in polymer matrices: Contemporary approaches and future advances, Composites: Part A 56 (2014) 103–126, https://doi.org/10.1016/j.compositesa.2013.10.001.
[48] W. Bauhofer, J.Z. Kovacs, A review and analysis of electrical percolation in carbon nanotube polymer composites, Compos. Sci. Technol. 69 (2009) 1486–1498, https://doi.org/10.1016/j.compscitech.2008.06.018.
[49] G. Massaglia, V. Margaria, M. Re Fiorentin, K. Pasha, A. Sacco, M. Castellino, A. Chiodoni, S. Bianco, F.C. Pirri, M. Quaglio, Nonwoven mats of N-doped carbon nanofibers as high-performing anodes in microbial fuel cells, Mater. Today Energy 16 (2020), 100385, https://doi.org/10.1016/j.mtener.2020.100385.
[50] M. Quaglio, S. Bianco, R. Castagna, M. Cocuzza, C.F. Pirri, Elastomeric nanocomposite based on carbon nanotubes for polymerase chain reaction device, Microelectron. Eng. 88 (2011) 1860–1863, https://doi.org/10.1016/j.mee.2011.01.032.
[51] T. Zhai, D. Li, G. Fei, H. Xia, Piezoresistive and compression resistance relaxation behavior of water blown carbon nanotube/polyurethane composite foam, Composit.: Part A 72 (2015) 108–114, https://doi.org/10.1016/j.compositesa.2015.02.003.
[52] J-H. Pu, X-J. Zha, M. Zhao, S. Li, R-Y. Bao, Z-Y. Liu, B-H. Xie, M-Bo Yang, Z. Guo, W. Yang, 2D end-to-end carbon nanotube conductive networks in polymer nanocomposites: a conceptual design to dramatically enhance the sensitivities of strain sensors, Nanoscale 10 (2018) 2191–2198, https://doi.org/10.1039/C7NR08077H.
[53] M. Amjadi, K.U. Kyung, I. Park, M. Sitti, Stretchable, skin-mountable, and wearable strain sensors and their potential applications: a review, Adv. Funct. Mater. 26 (2016) 1678–1698, https://doi.org/10.1002/adfm.201504755.
[54] Y. Lu, M.C. Biswas, Z Guo, J-W. Jeon, E.K. Wujcik, Biosens. Bioelectron. 123 (2019) 167–177, https://doi.org/10.1016/j.bios.2018.08.037.
[55] J.R. Garcia, D. O'Suilleabhain, H. Kaur, J.N. Coleman, A simple model relating gauge factor to filler loading in nanocomposite strain sensors, ACS Appl. Nano Mater. 4 (2021) 2876–2886, https://doi.org/10.1021/acsanm.1c00040.